Acta Cryst E CRYSTALLOGRAPHIC COMMUNICATIONS

ISSN 2056-9890

Crystal structure, Hirshfeld surface analysis and crystal voids of 4-nitrobenzo[*c*][1,2,5]selenadiazole

Atash V. Gurbanov,[a,b] Tuncer Hökelek,[c] Gunay Z. Mammadova,[d] Khudayar I. Hasanov,[e,f] Tahir A. Javadzade[g] and Alebel N. Belay[h]*

[a]Excellence Center, Baku State University, Z. Xalilov Str. 23, Az 1148 Baku, Azerbaijan, [b]Centro de Quimica Estrutural, Instituto Superior Tecnico, Universidade de Lisboa, Av. Rovisco Pais, 1049-001 Lisbon, Portugal, [c]Hacettepe University, Department of Physics, 06800 Beytepe-Ankara, Türkiye, [d]Department of Chemistry, Baku State University, Z. Khalilov Str. 23, Az 1148 Baku, Azerbaijan, [e]Western Caspian University, Istiglaliyyat Str. 31, AZ 1001 Baku, Azerbaijan, [f]Azerbaijan Medical University, Scientific Research Centre (SRC), A. Kasumzade Str. 14, AZ 1022 Baku, Azerbaijan, [g]Department of Chemistry and Chemical Engineering, Khazar University, Mahzati Str. 41, AZ 1096 Baku, Azerbaijan, and [h]Department of Chemistry, Bahir Dar University, PO Box 79, Bahir Dar, Ethiopia. *Correspondence e-mail: alebel.nibret@bdu.edu.et

Received 24 October 2024
Accepted 23 December 2024

Edited by F. Di Salvo, University of Buenos Aires, Argentina

Keywords: crystal structure; non-covalent interactions; chalcogen bond.

CCDC reference: 2412565

Supporting information: this article has supporting information at journals.iucr.org/e

The title molecule, $C_6H_3N_3O_2Se$, is almost planar. In the crystal, intermolecular C—H···O hydrogen bonds link the molecules into a network structure, enclosing $R_2^2(7)$ and $R_3^3(8)$ ring motifs, parallel to the *bc* plane. There are π–π interactions present with centroid-to-centroid distances of 3.746 (3) and 3.697 (3) Å. A Hirshfeld surface analysis of the crystal structure indicates that the most important contributions for the crystal packing are from H···O/O···H (19.6%), H···N/N···H (11.0%), H···Se/Se···H (8.5%), O···Se/Se···O (8.2%), H···H (7.4%), C···N/N···C (7.3%) and N···Se/Se···N (7.2%) interactions. Hydrogen bonding and van der Waals interactions are the dominant interactions in the crystal packing. The volume of the crystal voids and the percentage of free space were calculated to be 25.60 Å^3 and 3.73%, showing that there is no large cavity in the crystal.

1. Chemical context

Like other weak interactions, the chalcogen bond (ChB) has attracted considerable attention due to its various applications in synthesis, catalysis, crystal engineering, biochemical processes, molecular recognition, functional materials, *etc*. (Mahmudov *et al.*, 2017; Mahmudov *et al.*, 2022; Scilabra *et al.*, 2019). Both bond parameters, strength and directionality of ChB can be improved by variation of substituents, ChB atom (tunability), nucleophile, resonance and cooperation of weak interactions (Aliyeva *et al.*, 2024; Gurbanov *et al.*, 2020). For instance, due to cooperation of the ChB, the common four-membered Se_2N_2 aggregate of [1,2,5]selenadiazoles is well employed in materials chemistry (Hua *et al.*, 2020; Ho *et al.*, 2020; Tiekink, 2022). In this regard, we studied the *ortho*-NO_2 effect on the Se_2N_2 synthon of 4-nitrobenzo[*c*][1,2,5]selenadiazole aggregates. We provided herein a detailed synthesis and an examination of the molecular and crystal structures together with the Hirshfeld surface analysis and crystal voids of the title compound, (I).

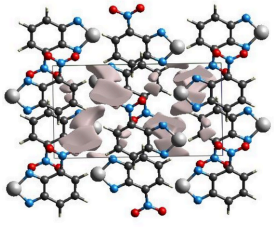

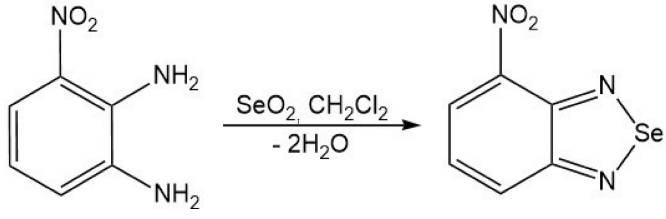

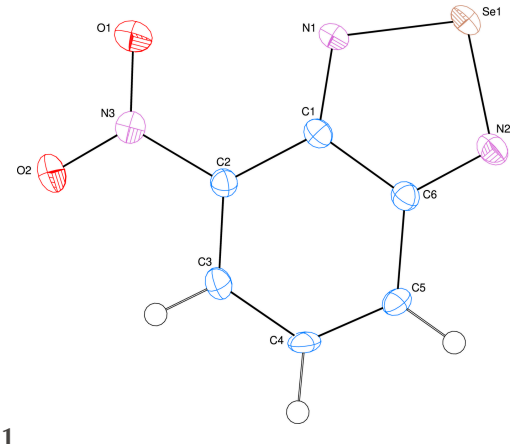

Figure 1
The title molecule with the atom-numbering scheme and 50% probability ellipsoids.

2. Structural commentary

The title compound (Fig. 1) is almost planar, with the planar *A* (C1–C6) and *B* (Se/N1/N2/C1/C6) rings oriented at a dihedral angle of *A*/*B* = 0.94 (15)°. Atoms N3, O1 and O2 are displaced by −0.004 (6), −0.024 (6) and 0.022 (6) Å, respectively, from the best least-squares plane of ring *A*. Hence, they are almost coplanar. There are no unusual bond distances or interbond angles in the molecule.

3. Supramolecular features

In the crystal, intermolecular C—H···O hydrogen bonds (Table 1) link the molecules into a network structure, enclosing $R_2^2(7)$ and $R_3^3(8)$ ring motifs (Fig. 2), parallel to the *bc* plane (Fig. 3). No C—H···π(ring) interactions are observed but there are two π–π interactions between the almost parallel *A* and *B* rings and also between the parallel *B* rings with centroid-to-centroid distances of 3.746 (3) and 3.697 (3) Å, respectively [*Cg*1···*Cg*2^{i} = 3.746 (3) Å with α = 0.91° and *Cg*2···*Cg*2^{i} = 3.697 (3) Å with α = 0.00° where *Cg*1 and *Cg*2 are the centroids of rings *A* and *B*, respectively; symmetry code: (i) −*x*, −*y*, 1 − *z*].

Table 1
Hydrogen-bond geometry (Å, °).

D—H···*A*	*D*—H	H···*A*	*D*···*A*	*D*—H···*A*
C4—H4···O2^{iv}	0.95	2.52	3.269 (7)	135
C5—H5···O1^{iii}	0.95	2.33	3.240 (7)	161

Symmetry codes: (iii) *x*, *y*, *z* + 1; (iv) *x*, $-y+\frac{3}{2}$, $z+\frac{1}{2}$.

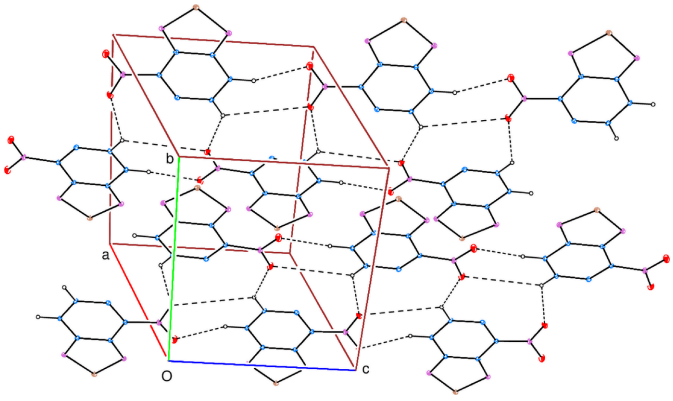

Figure 2
A partial packing diagram. Intermolecular C—H···O hydrogen bonds are shown by dashed lines.

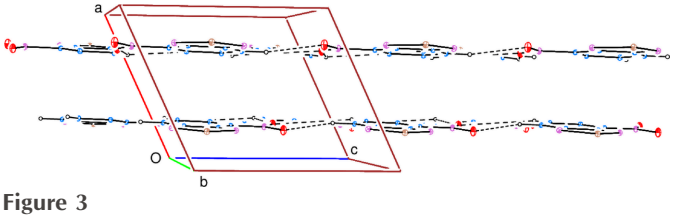

Figure 3
A partial packing diagram, viewed down the *b*-axis direction. Intermolecular C—H···O hydrogen bonds are shown by dashed lines.

4. Hirshfeld surface analysis

In order to visualize the intermolecular interactions, a Hirshfeld surface (HS) analysis (Hirshfeld, 1977; Spackman & Jayatilaka, 2009) was carried out using *Crystal Explorer 17.5* (Spackman *et al.*, 2021). In the HS plotted over d_{norm} (Fig. 4), the white areas indicate contacts with distances equal to the sum of van der Waals radii, and the red and blue colours indicate distances shorter (in close contact) or longer (distinct contact) than the van der Waals radii, respectively (Venkatesan *et al.*, 2016). The bright-red spots indicate their roles as the respective donors and/or acceptors. The shape-index surface can be used to identify characteristic packing modes, in particular, planar stacking arrangements and the presence of aromatic stacking interactions such as C—H···π and π–π interactions. C—H···π interactions are represented as red *p*-holes, which are related to the electron ring interactions between the CH groups and the centroid of the aromatic rings of neighbouring molecules. Fig. 5 clearly suggests that there

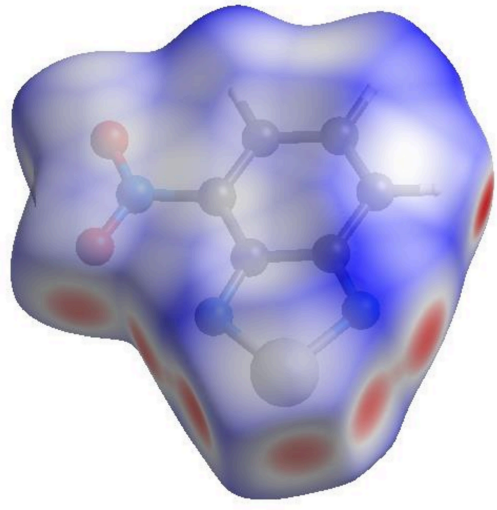

Figure 4
View of the three-dimensional Hirshfeld surface of the title compound plotted over d_{norm}.

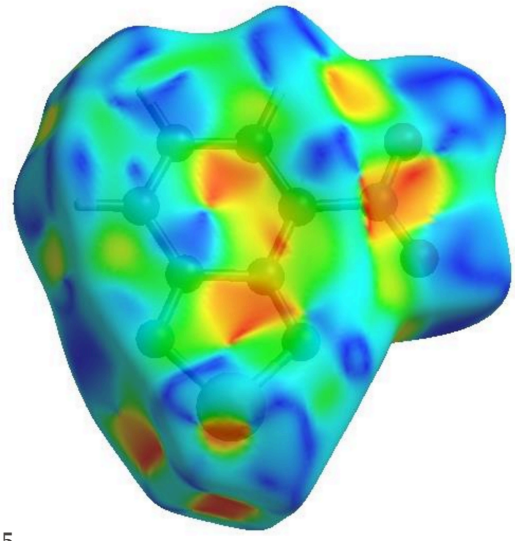

Figure 5
Hirshfeld surface of the title compound plotted over shape-index.

are no C—H···π interactions in (I). The shape-index is a tool for visualizing π–π stacking by the presence of adjacent red and blue triangles; if there are no adjacent red and/or blue triangles, then there are no π–π interactions. Fig. 5 clearly suggests that there are π–π interactions in (I). The overall two-dimensional fingerprint plot, Fig. 6*a*, and those delineated into H···O/O···H, H···N/N···H, H···Se/Se···H, O···Se/Se···O, H···H, C···N/N···C, N···Se/Se···N, N···O/O···N, C···O/O···C, H···C/C···H, C···C, N···N, O···O and C···Se/Se···C (McKinnon *et al.*, 2007) are illustrated in Fig. 6*b*–*o*, respectively, together with their relative contributions to the Hirshfeld surface. The most important interaction is H···O/O···H (Table 2) contributing 19.6% to the overall crystal packing, which is reflected in Fig. 6*b* as a pair of spikes with the tips at $d_e + d_i$ = 2.20 Å. The H···N/N···H contacts (Fig. 6*c*) make an 11.0% contribution to the HS and have the tips at $d_e + d_i$ = 3.46 Å. The H···Se/Se···H contacts (Fig. 6*d*; 8.5% contribution to the HS) have a pair of wings with the tips at $d_e + d_i$ = 3.34 Å. The pair of spikes for the O···Se/Se···O contacts (Table 2 and Fig. 6*e*), contributing 8.2% to the HS, have the tips at $d_e + d_i$ = 3.14 Å. The H···H interactions (Fig. 6*f*) contribute 7.4% to the HS with the tip at $d_e = d_i$ = 1.12 Å. The C···N/N···C (Fig. 6*g*), N···Se/Se···N (Table 2 and Fig. 6*h*) and N···O/O ···N (Table 2 and Fig. 6*i*) contacts contribute 7.3%, 7.2% and 6.9%, respectively, to the HS and are viewed as pairs of spikes with the tips at $d_e + d_i$ = 3.26, 3.08 and 3.04 Å, respectively. The C···O/ O···C contacts (Fig. 6*j*) make 6.4% contribution to the HS with the central point at $d_e = d_i$ = 1.72 Å. In the absence of C—H···π interactions, the H···C/C···H contacts, contributing 5.9% to the overall crystal packing, are reflected in Fig. 6*k* with the tips at $d_e + d_i$ = 3.46 Å. The C···C contacts (Fig. 6*l*) contributing 5.1% to the HS have a bullet-shaped distribution of points with the tip at $d_e = d_i$ = 1.69Å. Finally, the N···N (Table 2 and Fig. 6*m*), O···O (Fig. 6*n*) and C···Se/Se···C (Fig. 6*o*) contacts with 3.3%, 2.1% and 1.1% contributions, respectively, to the HS have very low densities.

Table 2
Selected interatomic distances (Å).

Se1···O1^{i}	3.140 (4)	O2···H3	2.37
Se1···N1^{i}	3.132 (5)	H4···O2^{iv}	2.52
Se1···N2^{ii}	3.079 (5)	N1···N3	3.012 (6)
O1···N1	2.709 (6)	N1···N2^{ii}	3.017 (6)
H5···O1^{iii}	2.33		

Symmetry codes: (i) $x, -y+\frac{1}{2}, z+\frac{1}{2}$; (ii) $x, -y+\frac{1}{2}, z-\frac{1}{2}$; (iii) $x, y, z+1$; (iv) $x, -y+\frac{3}{2}, z+\frac{1}{2}$.

The nearest neighbour coordination environment of a molecule can be determined from the colour patches on the HS based on how close to other molecules they are. The Hirshfeld surface representations with the function d_{norm} plotted onto the surface are shown for the H···O/O···H, H···N/N···H and H···Se/Se···H interactions in Fig. 7*a*–*c*, respectively.

The Hirshfeld surface analysis confirms the importance of H-atom contacts in establishing the packing. The large number of H···O/O···H, H···N/N···H and H···Se/Se···H interactions suggest that van der Waals interactions and hydrogen

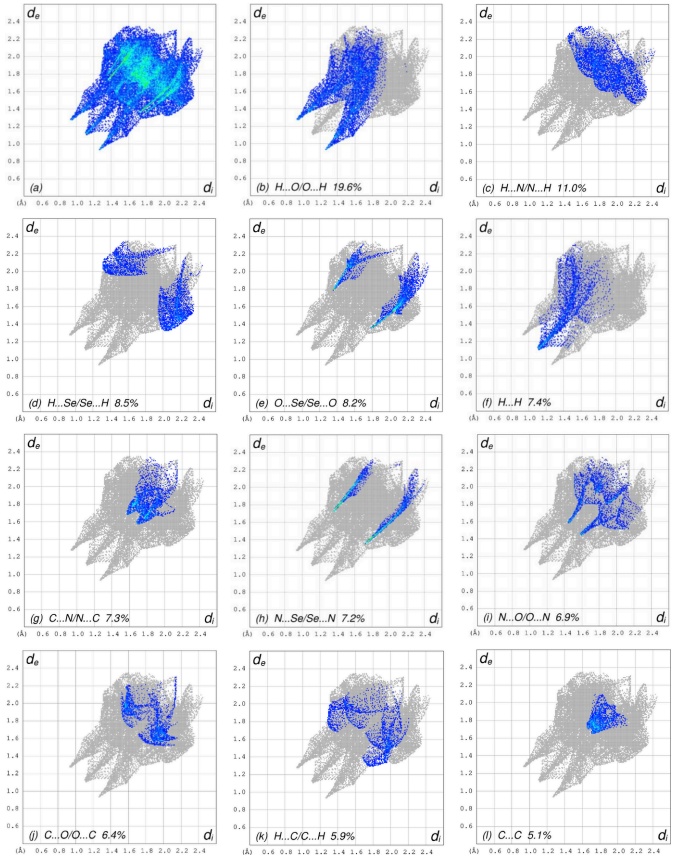

Figure 6
The full two-dimensional fingerprint plots for the title compound, showing (*a*) all interactions, and delineated into (*b*) H···O/O···H, (*c*) H···N/N···H, (*d*) H···Se/Se···H, (*e*) O···Se/Se···O, (*f*) H···H, (*g*) C···N/N···C, (*h*) N···Se/Se···N, (*i*) N···O/O···N, (*j*) C···O/O···C, (*k*) H···C/C ···H, (*l*) C···C, (*m*) N···N, (*n*) O···O and (*o*) C···Se/Se···C interactions. The d_i and d_e values are the closest internal and external distances (in Å) from given points on the Hirshfeld surface.

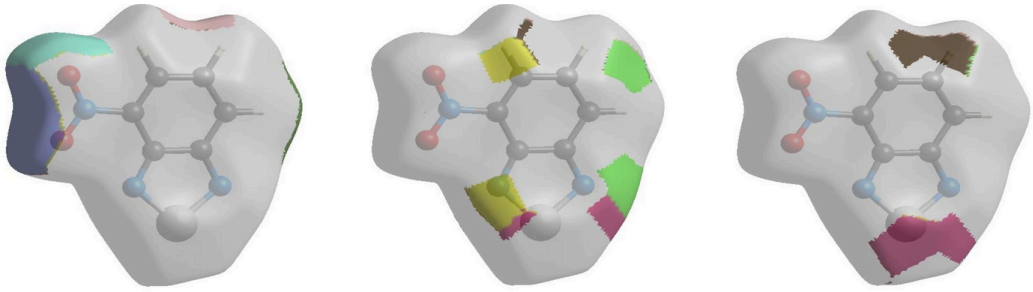

Figure 7
The Hirshfeld surface representations with the function d_{norm} plotted onto the surface for (*a*) H···O/O···H, (*b*) H···N/N···H and (*c*) H···Se/Se···H interactions.

bonding play the major roles in the crystal packing (Hathwar *et al.*, 2015).

5. Crystal voids

The strength of the crystal packing is important for determining the response to an applied mechanical force. If the crystal packing results in significant voids, the molecules are not tightly packed and a small amount of applied external mechanical force may easily break the crystal. To check the mechanical stability of the crystal, a void analysis was performed by adding up the electron densities of the spherically symmetric atoms contained in the asymmetric unit (Turner *et al.*, 2011). The void surface is defined as an isosurface of the procrystal electron density and is calculated for the whole unit cell where the void surface meets the boundary of the unit cell and capping faces are generated to create an enclosed volume. The volume of the crystal voids (Fig. 8*a*–*c*) and the percentage of free space in the unit cell are calculated as 25.60 Å^3 and 3.73%, respectively. Thus, the crystal packing appears compact and the mechanical stability should be substantial.

6. Database survey

A survey conducted of the Cambridge Structural Database (CSD, Version 5.45, last updated September 2024; Groom *et al.*, 2016) indicates that two molecules are similar to the title compound (I): (*rac*)-4-methyl-4-nitro-2,1,3-benzoselenadiazol-5(4*H*)-one, $C_7H_5N_3O_3Se$ (CSD refcode JURLAJ; Tian *et al.*, 1993) and 5-nitro-2,1,3-benzoselenadiazole, $C_6H_3N_3O_2Se$ (CSD refcode DOBWUQ; Aliyeva *et al.*, 2023).

7. Synthesis and crystallization

3-Nitrobenzene-1,2-diamine (10 mmol) and selenium dioxide (10 mmol) were dissolved in 25 ml of dichloromethane and stirred for 1 h at ambient temperature, and further refluxed for 1 h (Georges *et al.*, 2024). After cooling to room temperature, the solvent was evaporated under reduced pressure to give the reaction product. Crystals suitable for X-ray analysis were obtained by slow evaporation of a methanol solution. Yield 82% (based on SeO_2), yellow powder soluble in methanol, ethanol and DMSO. Analysis calculated for $C_6H_3N_3O_2Se$ (M_r = 228.07): C, 31.60; H, 1.33; N, 18.42. Found: C, 31.58, H,

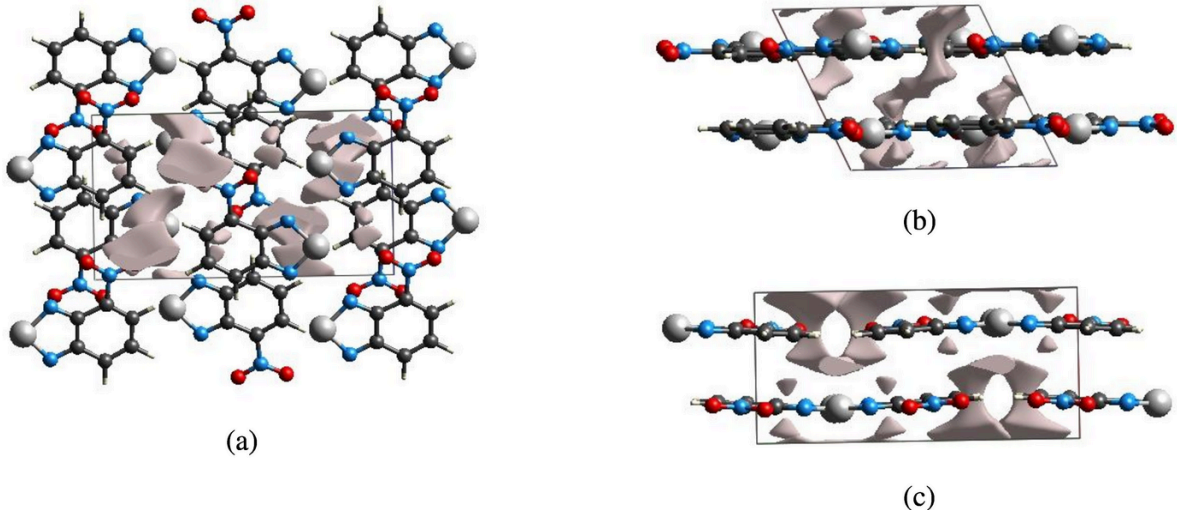

Figure 8
Graphical views of voids in the crystal packing of (I) (*a*) along the *a*-axis direction, (*b*) along the *b*-axis direction and (*c*) along the *c*-axis direction.

1.30; N, 18.40. ESI–MS (positive ion mode), *m*/*z*: 229.10 $[M_r + H]^{+\cdot}$ ^{1}H NMR (DMSO-d^6), δ: 7.72–8.46 (3H, Ar-H). ^{13}C NMR (DMSO-d^6), 126.4, 126.8, 129.4, 140.5, 149.9 and 159.9.

8. Refinement

Crystal data, data collection and structure refinement details are summarized in Table 3. The C-bond H atoms were positioned geometrically (C—H = 0.95 Å) and refined using a riding model with U_{iso}(H) = 1.2U_{eq}(C).

Acknowledgements

The authors' contributions are as follows. Conceptualization, AVG, TH and ANB; synthesis, AVG and GZM; X-ray analysis, AVG; writing (review and editing of the manuscript) AVG and TH; funding acquisition, AVG, GZM, KIH and TAJ; supervision, AVG, TH and ANB.

Funding information

This work was supported by the Fundaçao para a Ciencia e a Tecnologia (FCT, Portugal) , projects UIDB/00100/2020 (https://doi.org/10.54499/UIDB/00100/2020) and UIDP/00100/2020 (https://doi.org/10.54499/UIDP/00100/2020) of the Centro de Quimica Estrutural, and LA/P/0056/2020 (https://doi.org/10.54499/LA/P/0056/2020) of the Institute of Molecular Sciences, as well as Baku State University, Azerbaijan Medical University, Western Caspian University and Khazar University in Azerbaijan. TH is also grateful to Hacettepe University Scientific Research Project Unit (grant No. 013 D04 602 004).

Table 3
Experimental details.

Crystal data	
Chemical formula	$C_6H_3N_3O_2Se$
M_r	228.07
Crystal system, space group	Monoclinic, $P2_1/c$
Temperature (K)	150
a, b, c (Å)	7.0105 (4), 13.2765 (8), 8.1311 (5)
β (°)	114.808 (3)
V (Å^3)	686.96 (7)
Z	4
Radiation type	Mo $K\alpha$
μ (mm^{-1})	5.42
Crystal size (mm)	0.28 × 0.21 × 0.14
Data collection	
Diffractometer	Bruker APEXII CCD
Absorption correction	Multi-scan (*SADABS*; Krause *et al.*, 2015)
T_{min}, T_{max}	0.284, 0.473
No. of measured, independent and observed [$I > 2\sigma(I)$] reflections	5894, 1475, 1297
R_{int}	0.037
(sin $\theta/\lambda)_{max}$ (Å^{-1})	0.636
Refinement	
$R[F^2 > 2\sigma(F^2)]$, $wR(F^2)$, S	0.044, 0.104, 1.17
No. of reflections	1475
No. of parameters	109
H-atom treatment	H-atom parameters constrained
$\Delta\rho_{max}$, $\Delta\rho_{min}$ (e Å^{-3})	1.24, −1.27

Computer programs: *APEX4* and *SAINT* (Bruker, 2014), *SHELXT2019/1* (Sheldrick, 2015*a*), *SHELXL2019/1* (Sheldrick, 2015*b*) and *SHELXTL* (Sheldrick, 2008).

References

Aliyeva, V. A., Gurbanov, A. V., Guedes da Silva, M. F. C., Gomila, R. M., Frontera, A., Mahmudov, K. T. & Pombeiro, A. J. L. (2024). *Cryst. Growth Des.* **24**, 781–791.

Georges, T., Ovens, J. S. & Bryce, D. L. (2024). *Chem. A Eur. J.* e202402254.

Groom, C. R., Bruno, I. J., Lightfoot, M. P. & Ward, S. C. (2016). *Acta Cryst.* B**72**, 171–179.

Gurbanov, A. V., Kuznetsov, M. L., Mahmudov, K. T., Pombeiro, A. J. L. & Resnati, G. (2020). *Chem. A Eur. J.* **26**, 14833–14837.

Hathwar, V. R., Sist, M., Jørgensen, M. R. V., Mamakhel, A. H., Wang, X., Hoffmann, C. M., Sugimoto, K., Overgaard, J. & Iversen, B. B. (2015). *IUCrJ*, **2**, 563–574.

Hirshfeld, H. L. (1977). *Theor. Chim. Acta*, **44**, 129–138.

Ho, P. C., Wang, J. Z., Meloni, F. & Vargas-Baca, I. (2020). *Coord. Chem. Rev.* **422**, 213464.

Hua, B., Zhang, C., Zhou, W., Shao, L., Wang, Z., Wang, L., Zhu, H. & Huang, F. (2020). *J. Am. Chem. Soc.* **142**, 16557–16561.

Krause, L., Herbst-Irmer, R., Sheldrick, G. M. & Stalke, D. (2015). *J. Appl. Cryst.* **48**, 3–10.

Mahmudov, K. T., Gurbanov, A. V., Aliyeva, V. A., Guedes da Silva, M. F. C., Resnati, G. & Pombeiro, A. J. L. (2022). *Coord. Chem. Rev.* **464**, 214556.

Mahmudov, K. T., Kopylovich, M. N., Guedes da Silva, M. F. C. & Pombeiro, A. J. L. (2017). *Dalton Trans.* **46**, 10121–10138.

McKinnon, J. J., Jayatilaka, D. & Spackman, M. A. (2007). *Chem. Commun.* pp. 3814.

Scilabra, P., Terraneo, G. & Resnati, G. (2019). *Acc. Chem. Res.* **52**, 1313–1324.

Sheldrick, G. M. (2008). *Acta Cryst.* A**64**, 112–122.

Sheldrick, G. M. (2015*a*). *Acta Cryst.* A**71**, 3–8.

Sheldrick, G. M. (2015*b*). *Acta Cryst.* C**71**, 3–8.

Spackman, M. A. & Jayatilaka, D. (2009). *CrystEngComm*, **11**, 19–32.

Spackman, P. R., Turner, M. J., McKinnon, J. J., Wolff, S. K., Grimwood, D. J., Jayatilaka, D. & Spackman, M. A. (2021). *J. Appl. Cryst.* **54**, 1006–1011.

Tian, W., Grivas, S. & Olsson, K. (1993). *J. Chem. Soc. Perkin Trans. 1*, pp. 257.

Tiekink, E. R. T. (2022). *CrystEngComm*, **25**, 9–39.

Turner, M. J., McKinnon, J. J., Jayatilaka, D. & Spackman, M. A. (2011). *CrystEngComm*, **13**, 1804–1813.

Venkatesan, P., Thamotharan, S., Ilangovan, A., Liang, H. & Sundius, T. (2016). *Spectrochim. Acta A Mol. Biomol. Spectrosc.* **153**, 625–636.

supporting information

Acta Cryst. (2025). E**81**, 99-103 [https://doi.org/10.1107/S2056989024012398]

Crystal structure, Hirshfeld surface analysis and crystal voids of 4-nitrobenzo[*c*][1,2,5]selenadiazole

Atash V. Gurbanov, Tuncer Hökelek, Gunay Z. Mammadova, Khudayar I. Hasanov, Tahir A. Javadzade and Alebel N. Belay

Computing details

4-Nitrobenzo[*c*][1,2,5]selenadiazole

Crystal data

$C_6H_3N_3O_2Se$
$M_r = 228.07$
Monoclinic, $P2_1/c$
$a = 7.0105$ (4) Å
$b = 13.2765$ (8) Å
$c = 8.1311$ (5) Å
$\beta = 114.808$ (3)°
$V = 686.96$ (7) Å^3
$Z = 4$
$F(000) = 440$
$D_x = 2.205$ Mg m^{-3}
Mo $K\alpha$ radiation, $\lambda = 0.71073$ Å
Cell parameters from 2556 reflections
$\theta = 3.1$–26.7°
$\mu = 5.42$ mm^{-1}
$T = 150$ K
Prism, yellow
0.28 × 0.21 × 0.14 mm

Data collection

Bruker APEXII CCD diffractometer
φ and ω scans
Absorption correction: multi-scan (SADABS; Krause *et al.*, 2015)
$T_{min} = 0.284$, $T_{max} = 0.473$
5894 measured reflections
1475 independent reflections
1297 reflections with $I > 2\sigma(I)$
$R_{int} = 0.037$
$\theta_{max} = 26.9°$, $\theta_{min} = 3.1°$
$h = -8 \rightarrow 8$
$k = -16 \rightarrow 16$
$l = -10 \rightarrow 10$

Refinement

Refinement on F^2
Least-squares matrix: full
$R[F^2 > 2\sigma(F^2)] = 0.044$
$wR(F^2) = 0.104$
$S = 1.17$
1475 reflections
109 parameters
0 restraints
Primary atom site location: structure-invariant direct methods
Secondary atom site location: difference Fourier map
Hydrogen site location: inferred from neighbouring sites
H-atom parameters constrained
$w = 1/[\sigma^2(F_o^2) + 6.1884P]$ where $P = (F_o^2 + 2F_c^2)/3$
$(\Delta/\sigma)_{max} < 0.001$
$\Delta\rho_{max} = 1.24$ e Å^{-3}
$\Delta\rho_{min} = -1.27$ e Å^{-3}

Special details

Geometry. All esds (except the esd in the dihedral angle between two l.s. planes) are estimated using the full covariance matrix. The cell esds are taken into account individually in the estimation of esds in distances, angles and torsion angles; correlations between esds in cell parameters are only used when they are defined by crystal symmetry. An approximate (isotropic) treatment of cell esds is used for estimating esds involving l.s. planes.

Fractional atomic coordinates and isotropic or equivalent isotropic displacement parameters (Å²)

	x	*y*	*z*	U_{iso}*/U_{eq}
Se1	0.77441 (9)	0.25835 (4)	0.82143 (8)	0.01947 (18)
O1	0.7737 (8)	0.4739 (3)	0.3944 (6)	0.0372 (11)
O2	0.7408 (8)	0.6348 (3)	0.4079 (6)	0.0324 (11)
N1	0.7713 (7)	0.3520 (3)	0.6607 (6)	0.0179 (10)
N2	0.7564 (7)	0.3476 (3)	0.9783 (6)	0.0198 (10)
N3	0.7548 (8)	0.5496 (3)	0.4731 (6)	0.0219 (10)
C1	0.7570 (8)	0.4405 (4)	0.7304 (7)	0.0152 (10)
C2	0.7477 (8)	0.5380 (4)	0.6503 (7)	0.0155 (10)
C3	0.7288 (8)	0.6233 (4)	0.7359 (7)	0.0175 (11)
H3	0.720824	0.686805	0.679574	0.021*
C4	0.7207 (8)	0.6192 (4)	0.9056 (7)	0.0174 (11)
H4	0.707675	0.680103	0.961342	0.021*
C5	0.7310 (8)	0.5300 (4)	0.9926 (7)	0.0164 (10)
H5	0.726556	0.528392	1.107708	0.020*
C6	0.7487 (8)	0.4387 (4)	0.9056 (7)	0.0161 (10)

Atomic displacement parameters (Å²)

	U^{11}	U^{22}	U^{33}	U^{12}	U^{13}	U^{23}
Se1	0.0249 (3)	0.0107 (2)	0.0233 (3)	0.0001 (2)	0.0106 (2)	0.0017 (2)
O1	0.066 (3)	0.019 (2)	0.034 (3)	0.001 (2)	0.029 (2)	−0.0030 (18)
O2	0.054 (3)	0.019 (2)	0.029 (2)	0.0017 (19)	0.022 (2)	0.0081 (17)
N1	0.023 (3)	0.012 (2)	0.020 (2)	0.0017 (17)	0.009 (2)	−0.0001 (17)
N2	0.022 (2)	0.014 (2)	0.024 (3)	0.0000 (17)	0.011 (2)	0.0018 (18)
N3	0.028 (3)	0.020 (2)	0.020 (3)	0.0003 (19)	0.012 (2)	0.0011 (19)
C1	0.013 (2)	0.014 (2)	0.018 (3)	−0.0010 (18)	0.006 (2)	0.0004 (19)
C2	0.017 (3)	0.015 (2)	0.017 (3)	0.0001 (19)	0.008 (2)	0.0010 (19)
C3	0.019 (3)	0.015 (2)	0.017 (3)	0.001 (2)	0.006 (2)	0.003 (2)
C4	0.022 (3)	0.014 (2)	0.019 (3)	0.001 (2)	0.012 (2)	−0.0055 (19)
C5	0.019 (3)	0.018 (2)	0.015 (3)	0.001 (2)	0.010 (2)	−0.002 (2)
C6	0.016 (3)	0.015 (2)	0.018 (3)	0.0005 (19)	0.009 (2)	0.0011 (19)

Geometric parameters (Å, º)

Se1—N2	1.784 (5)	C1—C6	1.450 (7)
Se1—N1	1.797 (4)	C2—C3	1.364 (7)
O1—N3	1.228 (6)	C3—C4	1.406 (7)
O2—N3	1.235 (6)	C3—H3	0.9500
N1—C1	1.327 (6)	C4—C5	1.366 (7)

N2—C6	1.338 (7)	C4—H4	0.9500
N3—C2	1.471 (7)	C5—C6	1.434 (7)
C1—C2	1.439 (7)	C5—H5	0.9500
Se1···O1^{i}	3.140 (4)	O2···H3	2.37
Se1···N1^{i}	3.132 (5)	H4···O2^{iv}	2.52
Se1···N2^{ii}	3.079 (5)	N1···N3	3.012 (6)
O1···N1	2.709 (6)	N1···N2^{ii}	3.017 (6)
H5···O1^{iii}	2.33		
N2—Se1—N1	94.46 (19)	C2—C3—C4	121.4 (5)
C1—N1—Se1	106.4 (3)	C2—C3—H3	119.3
C6—N2—Se1	106.7 (4)	C4—C3—H3	119.3
O1—N3—O2	122.2 (5)	C5—C4—C3	121.8 (5)
O1—N3—C2	118.7 (4)	C5—C4—H4	119.1
O2—N3—C2	119.1 (4)	C3—C4—H4	119.1
N1—C1—C2	126.9 (5)	C4—C5—C6	118.3 (5)
N1—C1—C6	116.5 (5)	C4—C5—H5	120.8
C2—C1—C6	116.5 (4)	C6—C5—H5	120.8
C3—C2—C1	120.7 (5)	N2—C6—C5	122.8 (5)
C3—C2—N3	117.6 (4)	N2—C6—C1	116.0 (5)
C1—C2—N3	121.6 (4)	C5—C6—C1	121.2 (5)
N2—Se1—N1—C1	−0.2 (4)	C1—C2—C3—C4	0.9 (8)
N1—Se1—N2—C6	0.2 (4)	N3—C2—C3—C4	180.0 (5)
Se1—N1—C1—C2	−179.5 (4)	C2—C3—C4—C5	−0.1 (9)
Se1—N1—C1—C6	0.2 (6)	C3—C4—C5—C6	−0.5 (8)
N1—C1—C2—C3	178.7 (5)	Se1—N2—C6—C5	179.2 (4)
C6—C1—C2—C3	−1.0 (7)	Se1—N2—C6—C1	−0.1 (6)
N1—C1—C2—N3	−0.3 (8)	C4—C5—C6—N2	−178.9 (5)
C6—C1—C2—N3	180.0 (5)	C4—C5—C6—C1	0.4 (8)
O1—N3—C2—C3	179.4 (5)	N1—C1—C6—N2	0.0 (7)
O2—N3—C2—C3	−0.9 (8)	C2—C1—C6—N2	179.7 (5)
O1—N3—C2—C1	−1.6 (8)	N1—C1—C6—C5	−179.4 (5)
O2—N3—C2—C1	178.1 (5)	C2—C1—C6—C5	0.4 (7)

Symmetry codes: (i) x, $-y+1/2$, $z+1/2$; (ii) x, $-y+1/2$, $z-1/2$; (iii) x, y, $z+1$; (iv) x, $-y+3/2$, $z+1/2$.

Hydrogen-bond geometry (Å, º)

D—H···*A*	*D*—H	H···*A*	*D*···*A*	*D*—H···*A*
C4—H4···O2^{iv}	0.95	2.52	3.269 (7)	135
C5—H5···O1^{iii}	0.95	2.33	3.240 (7)	161

Symmetry codes: (iii) x, y, $z+1$; (iv) x, $-y+3/2$, $z+1/2$.